Computers and Structures 87 (2009) 751–757

Contents lists available at ScienceDirect

Computers and Structures

journal homepage: www.elsevier.com/locate/compstruc

Some remarks on quadrilateral mixed finite elements

Daniele Boffi [a,*], Lucia Gastaldi [b]

[a] Dipartimento di Matematica, Università di Pavia, Via Ferrata 1, Pavia, Italy
[b] Dipartimento di Matematica, Università di Brescia, Via Valotti 9, Brescia, Italy

ARTICLE INFO

Article history:
Received 5 June 2008
Accepted 1 December 2008
Available online 10 January 2009

Keywords:
Quadrilateral
Finite elements
Approximation
Mimetic finite differences
Mixed finite elements

ABSTRACT

It is well known that quadrilateral finite elements may produce unsatisfactory results when used on distorted meshes. It turns out that many commonly used finite elements achieve suboptimal convergence properties on distorted quadrilaterals; among such elements we recall in particular serendipity (trunk) scalar elements and basically all vectorial elements for the approximation of problems involving the functional space $H(\mathrm{div})$ (like Raviart–Thomas or Brezzi–Douglas–Marini spaces for Darcy flow). In two space dimensions, a similar remark applies to edge finite elements for the approximation of Maxwell's problems involving the space $H(\mathrm{curl})$.

On the other hand, mimetic finite differences have become popular for the approximation of problems involving $H(\mathrm{div})$ on very general geometries.

The aim of this paper is to show how to use the ideas of mimetic finite differences for the stabilization of Raviart–Thomas element on general quadrilateral meshes. It turns out that such stabilization can be performed by a slight modification of the standard Raviart–Thomas element which does not increase significantly the computational cost of the original scheme.

1. Introduction

In this paper we deal with the mixed finite element approximation of viscous flow problems on general quadrilateral meshes. It is well known that standard finite elements for the discretization of $H(\mathrm{div};\Omega)$, like Raviart–Thomas (RT), Brezzi–Douglas–Marini (BDM), or Brezzi–Douglas–Fortin–Marini (BDFM), achieve suboptimal approximation properties on general quadrilateral meshes. According to Arnold et al. [1], two-dimensional RT elements are optimal in $L^2(\Omega)$ but suboptimal by one order in $H(\mathrm{div};\Omega)$, while the other known families of finite elements suffer from a substantial reduction in their order of approximation both in $L^2(\Omega)$ and $H(\mathrm{div};\Omega)$. The three-dimensional situation is even worse: for instance, lowest-order RT elements are not converging in $L^2(\Omega)$. We refer the interested reader to Section 6 where a detailed comparison between the approximation properties of different mixed finite element spaces is carried out (see, in particular, Tables 6 and 7).

The modeling of acoustic or fluid–structure interaction systems is often reduced to problems which involve the "$\nabla\mathrm{div}$" operator (see, for instance [3,26,27,5,9]). It turns out that on triangular or rectangular meshes the eigensolutions of mixed Laplace equation coincide with those of "$\nabla\mathrm{div}$" operator (up to the approximation of the infinite dimensional kernel). However, on quadrilateral meshes, the equivalence is no longer true and the two problems have to be studied separately unless an appropriate choice of the finite element spaces is made. This issue will be discussed and made more precise in Section 2.

Mimetic finite differences technique is a powerful tool for the analysis of viscous flow problems on very general geometries (see, for instance [24,21,14,16,13,15]). The method allows for flexible triangulations of polygonal or polyhedral domains; the elements can be general polygons or polyhedrons with any number of (possible curved) sides/faces. Since on symplectic triangulations it is well-known that particular choices of mimetic finite differences can be interpreted as mixed finite elements (see [6,7]), it is natural to study the behavior of mimetic finite differences of quadrilateral meshes and investigate whether this can be interpreted as a modification of standard quadrilateral finite elements. The aim of this paper is to discuss such correspondence; it turns out that a suitable modification of standard RT element (see also [25]) can be analyzed within the framework of mimetic finite differences. This remark allows us to prove optimal approximation properties for the modified mixed element and its optimal performances for the solution of the source and the eigenvalue problem (see [11]).

The new contribution of the present paper is two-folds. From one side, we present an explicit derivation of the so called lifting (or reconstruction) operator in the framework of mimetic finite differences (see [13]); from the other side, the equivalence between the modified RT element and a mimetic finite difference formulation allows for a complete and rigorous mathematical analysis of the original scheme presented in [25]. Moreover, we hope that

* Corresponding author.
E-mail address: daniele.boffi@unipv.it (D. Boffi).

0045-7949/$ - see front matter © 2008 Elsevier Ltd. All rights reserved.
doi:10.1016/j.compstruc.2008.12.006

such equivalence can prove useful for the extension of the present result to the three-dimensional situation for which, so far, no available finite element schemes are present.

The structure of the paper is as follows: Section 2 sets the problems under consideration, discusses the links between the source and the eigenvalue problems, and recalls the main properties of RT approximation. Section 3 summarizes the main theory about mimetic finite differences applied to the problem of interest. Section 4 explains the modification of RT element presented in [25] and shows how it fits within the framework of mimetic finite differences. Some numerical results are presented in Section 5: the suboptimal performances of standard RT elements on distorted quadrilateral meshes are demonstrated together with the good behavior of the proposed modification.

Finally, a concluding remark summarizes the approximation properties for the most important finite element spaces for the approximation of $H(\mathrm{div};\Omega)$ and compare them with the element analyzed in this paper.

2. Raviart–Thomas elements for viscous flow

We are interested in the numerical solution to the following problem: find the velocity field $\mathbf{u}$ and the pressure p which satisfy

$$\begin{cases} \mathbf{u} = \mathbb{K}\nabla p & \text{in } \Omega, \\ \mathrm{div}\mathbf{u} = -f & \text{in } \Omega, \\ \mathbf{u}\cdot\mathbf{n} = 0 & \text{on } \partial\Omega, \end{cases}$$

where Ω is a polygonal domain in $\mathbb{R}^2$, $\mathbf{n}$ the outward unit normal vector to $\partial\Omega$, and $\mathbb{K}\in\mathbb{R}^{2\times 2}$ is a symmetric uniformly positive definite tensor representing the rock permeability divided by the fluid viscosity. We assume that the compatibility condition

$$\int_\Omega f\,dx = 0$$

is satisfied.

We consider the space $\mathbf{V} = \mathrm{H}_0(\mathrm{div};\Omega)$ of vectorfields $\mathbf{v}$ in $L^2(\Omega)^2$ with $\mathrm{div}\mathbf{v}$ in $L^2(\Omega)$ and vanishing normal component along $\partial\Omega$, and the space $Q = L^2_0(\Omega)$ of functions with zero mean value in Ω. A variational formulation of our problem reads: find $\mathbf{u}\in\mathbf{V}$ and $p\in Q$ such that

$$\begin{cases} (\mathbb{K}^{-1}\mathbf{u},\mathbf{v}) + (\mathrm{div}\mathbf{v},p) = 0 & \forall\mathbf{v}\in\mathbf{V}, \\ (\mathrm{div}\mathbf{u},q) = -(f,q) & \forall q\in Q. \end{cases} \tag{1}$$

It is well-known that a finite element discretization of (1) can be performed by means of RT elements. We will discuss the case of quadrilateral finite elements of lowest order. Denoting by $\mathbf{V}_h\subset\mathbf{V}$ and $Q_h\subset Q$ our finite element spaces, the discrete counterpart of (1) reads: find $\mathbf{u}_h\in\mathbf{V}_h$ and $p_h\in Q_h$ such that

$$\begin{cases} (\mathbb{K}^{-1}\mathbf{u}_h,\mathbf{v}) + (\mathrm{div}\mathbf{v},p_h) = 0 & \forall\mathbf{v}\in\mathbf{V}_h, \\ (\mathrm{div}\mathbf{u}_h,q) = -(f,q) & \forall q\in Q_h. \end{cases} \tag{2}$$

It has been shown in [1] that standard RT element on general quadrilateral meshes does not achieve optimal approximation properties. More precisely, on meshes of parallelograms (i.e., the mappings from the reference element to the actual ones are affine), the error estimates for problems (1) and (2) are

$$\|\mathbf{u}-\mathbf{u}_h\|_{L^2(\Omega)} \leqslant Ch\|\mathbf{u}\|_{H^1(\Omega)},$$
$$\|\mathrm{div}(\mathbf{u}-\mathbf{u}_h)\|_{L^2(\Omega)} \leqslant Ch\|\mathrm{div}\mathbf{u}\|_{H^1(\Omega)},$$
$$\|p-p_h\|_{L^2(\Omega)} \leqslant Ch\|p\|_{H^2(\Omega)}.$$

On the other hand, on general quadrilateral meshes (i.e., the mappings from the reference element to the actual ones are bilinear), the error in the approximation of $\mathrm{div}\mathbf{u}$ does not converge to zero. Actually, this suboptimal estimate is not a big deal for the problem we are discussing, since we already know that $\mathrm{div}\mathbf{u}$ is equal to $-f$. However, the situation is much worse in 3D, where also the error in $\mathbf{u}$ does not converge in the L^2-norm, or for other families of 2D mixed elements like BDM or BDFM. We refer the interested reader to Arnold et al. [1] for more details.

The suboptimal approximation properties of mixed finite elements on general quadrilateral meshes affect the solution to the following eigenvalue problem: find $\lambda\in\mathbb{R}$ and $\mathbf{u}\in\mathbf{V}$ with $\mathbf{u}\neq\mathbf{0}$ such that

$$(\mathrm{div}\mathbf{u},\mathrm{div}\mathbf{v}) = \lambda(\mathbb{K}^{-1}\mathbf{u},\mathbf{v}) \quad \forall\mathbf{v}\in\mathbf{V}. \tag{3}$$

Problem (3), which has been studied by several authors in the modeling and in the numerical approximation of fluid–structure interactions (see, for instance [3,5,26,27,20] is closely related to (1)). Actually, it can be shown that the solutions to (3) are exactly the same as those of the eigenvalue problem associated to (1) with the addition of $\lambda = 0$ which has an infinite dimensional eigenspace corresponding to the kernel of the divergence operator. This equivalence has been proved in [10] in a different setting related to Maxwell's equations. It has been shown in [4] and, in an equivalent setting in [12], that the Galerkin approximation to (3) by means of lowest-order RT element does not converge to the continuous solutions on general (distorted) quadrilateral meshes.

At discrete level, the equivalence between the eigenvalue problem associated with (2) and the discretization of (3) is true only if $\mathrm{div}\mathbf{V}_h = Q_h$. This equality is not valid on general quadrilateral meshes, if $\mathbf{V}_h$ is the lowest-order RT space and Q_h is, as usual, made of piecewise constant functions. Namely, it follows from the properties of the Piola transform that the divergence of a vectorfield in $\mathbf{V}_h$ is constant in a generic element K if and only if the Jacobian of the mapping from the reference element to K is constant, which implies that K is a parallelogram.

In Section 4, we shall present a modification of RT element in order to have $\mathrm{div}\mathbf{v}$ piecewise constant for $\mathbf{v}\in\mathbf{V}_h$, so that the equality $\mathrm{div}\mathbf{V}_h = Q_h$ will be satisfied. This important property, together with appropriate approximation estimates, will allow us to show optimal convergence for the problem under consideration.

The idea of enforcing a constant divergence for a lowest-order mixed element has been used also in [23] where a mixed space is constructed by decomposing a general polygonal element into subtriangles, by considering RT elements on the triangular submesh, and by eliminating the additional degrees of freedom in order to have piecewise constant divergence on the original mesh.

3. Mimetic finite differences for viscous flow

Mimetic finite differences have become a very popular tool for the approximation of Darcy flow problems on very general geometries and meshes. We refer the interested reader to Shashkov [24] and Hyman and Shashkov [21]; we are going to use the setting of Brezzi et al. [14,16,13,15] where recent developments on this topic have been presented.

We recall here the basic definitions and the main features of this technique. We are going to use a two-dimensional setting, since we are interested mainly on quadrilateral meshes, but we notice that mimetic finite differences are performing well also in three-dimensional domains and curved element faces are allowed as well. In particular, we are following the approach of Brezzi et al. [13], which the interested reader is referred to for more details.

A polygonal domain is decomposed into very general polygonal elements. As usual we associate with the mesh a parameter h (tending to zero) which is related to the maximum size of the elements. With each element E is associated the space $\mathbf{X}^h_E = \mathbb{R}^{k_E}$, where k_E is the number of sides of E. If we are given a generic ele-

ment $\mathbf{G}_E \in \mathbf{X}_E^h$, we denote by G_E^e its component related to the edge e of E. The meaning of the constant G_E^e is to *mimic* the normal component of a vectorfield along e. The velocity space $\mathbf{X}^h$ is then given by the following properties: the dimension of $\mathbf{X}^h$ is the number of internal edges of our mesh; the restriction of $\mathbf{X}^h$ to the element E is equal to $\mathbf{X}_E^h$; the following continuity assumption is made:

$$G_{E_1}^e = -G_{E_2}^e$$

for each edge e shared by two elements E_1 and E_2; finally the boundary conditions are accounted for by taking $G_E^e = 0$ for any boundary edge e.

Remark 1. One of the main differences between the space $\mathbf{X}^h$ and a standard finite element space is that a velocity field is discretized in $\mathbf{X}^h$ by means of its normal components along the boundaries of each element and not in the interior of the elements.

The pressure space $Q^h = Q_h$ is the same as in the previous section (piecewise constant functions).

Suitable scalar products are defined in $\mathbf{X}^h$ and Q^h. More precisely,

$$[p,q]_{Q^h} = \sum_E p_E q_E |E| \quad \forall p,q \in Q^h,$$

where p_E denotes the restriction of p to E and $|E|$ the area of E. It is clear that we have just used the standard L^2 scalar product.

The scalar product in $\mathbf{X}^h$ is

$$[\mathbf{F},\mathbf{G}]_{\mathbf{X}^h} = \sum_E [\mathbf{F}_E,\mathbf{G}_E]_E \quad \forall \mathbf{F},\mathbf{G} \in \mathbf{X}^h,$$

where

$$[\mathbf{F}_E,\mathbf{G}_E]_E = \sum_{r,s=1}^{k_E} \mathbb{M}_{E,r,s} F_E^{e_r} G_E^{e_s} \tag{4}$$

for a suitable symmetric and positive definite matrix $\mathbb{M}_E$.

Remark 2. The choice of $\mathbb{M}_E$ is crucial for the definition of our method. The scalar product in $\mathbf{X}^h$ should *mimic* the weighted L^2 scalar product for vectorfields which takes into account the presence of the matrix $\mathbb{K}$.

The next step is the definition of suitable discrete divergence and gradient operators: $\mathscr{DIV}^h\mathbf{G}$ is the element of Q^h which satisfies

$$(\mathscr{DIV}^h\mathbf{G})_E = \frac{1}{|E|}\sum_{r=1}^{k_E} G_E^{e_r}|e_r|,$$

where $|e|$ denotes the length of e. It is clear that the definition of $\mathscr{DIV}^h$ is driven by the Green formula. A weak gradient operator $\mathscr{GRAD}^h p$ can be defined as the adjoint of $\mathscr{DIV}^h$ by means of the discrete flux as follows

$$[\mathbf{F},\mathscr{GRAD}^h p]_{\mathbf{X}^h} = -[\mathscr{DIV}^h\mathbf{F},p]_{Q^h} \quad \forall p \in Q_h,\ \forall \mathbf{F} \in \mathbf{X}^h.$$

Finally, the mimetic discrete version of Darcy problem (1) can be written as follows: let $f^I \in Q^h$ be defined as

$$f_E^I = \frac{1}{|E|}\int_E f(x)dx,$$

then we look for $\mathbf{F} \in \mathbf{X}^h$ and $p \in Q^h$ such that

$$\begin{aligned} &\mathbf{F} = \mathscr{GRAD}^h p^h, \\ &\mathscr{DIV}^h\mathbf{F} = -f^I. \end{aligned} \tag{5}$$

Remark 3. Formulation (5) has to be completed by a suitable definition of the scalar product in $\mathbf{X}^h$ which is a main ingredient for the definition of the operator $\mathscr{GRAD}^h$.

The recent literature is very active on designing suitable scalar products: one of the main ideas is to prove that particular choices for $\mathbb{M}_E$ are associated to a lifting operator. Indeed, if we are given a lifting operator $\mathscr{R}_E : \mathbf{X}_E^h \to L^2(E)$ then scalar product can be computed by

$$[\mathbf{F}_E,\mathbf{G}_E]_E = \int_E \mathbb{K}^{-1}\mathscr{R}_E(\mathbf{F}_E)\cdot\mathscr{R}_E(\mathbf{G}_E)dx. \tag{6}$$

In particular, if E is a triangle, then $\mathscr{R}_E$ can be obtained by standard *lowest-order* RT (or BDM, etc.) finite element shape functions.

In practice, one wants to use the properties of the lifting operator *without* actually constructing the lifting operator itself.

For the error analysis of mimetic approximation of Darcy flow, the following definitions will be useful.

Definition 1. The local scalar product $[\cdot,\cdot]_E$ is said to be *stable* if there exist constants s_* and s^* such that

$$s_* \sum_e (G_E^e)^2|E| \leqslant [\mathbf{G}_E,\mathbf{G}_E]_E \leqslant s^* \sum_e (G_E^e)^2|E|. \tag{7}$$

Definition 2. The local scalar product $[\cdot,\cdot]_E$ is said to be *consistent* if

$$[(\widetilde{\mathbb{K}}\nabla q^1)^I,\mathbf{G}_E]_E = \int_{\partial E} q^1\mathbf{G}_E\cdot\mathbf{n}ds - \int_E q^1(\mathscr{DIV}^h\mathbf{G})_E dx \tag{8}$$

where $(\cdot)^I$ denotes an interpolation operator from vectorfields to $\mathbf{X}^h$ and $\widetilde{\mathbb{K}}$ is a constant matrix on E such that

$$\sup_{x\in E}\sup_{i,j}|\{\mathbb{K}(x)\}_{i,j} - \{\widetilde{\mathbb{K}}\}_{i,j}| \leqslant Ch_E$$

with C independent of E and h_E denoting the diameter of E.

Definition 3. An operator $\mathscr{R}_E : \mathbf{X}_E^h \to L^2(E)$ is said to be a P_0-*compatible lifting* if:

(1) $\mathscr{R}_E(G_E)|_e \cdot \mathbf{n}_e = G_E^e$ for all edges e of E;
(2) $\mathrm{div}\mathscr{R}_e(G_E)$ is constant for any $G_E \in \mathbf{X}_E^h$;
(3) for any constant vector $\mathbf{c}$, given $G_E \in \mathbf{X}_E^h$ such that $G_E^e = \mathbf{c}\cdot\mathbf{n}_e$ for all edges e of E, then $\mathscr{R}_E(G_E) = \mathbf{c}$;

where $\mathbf{n}_e$ is the outward normal unit vector associated with the edge e.

Remark 4. Theorem 5.1 of [13] states that, if there exists a P_0-compatible lifting, then the local scalar product $[\cdot,\cdot]_E$ is consistent in the spirit of (8).

The error estimates for the variable $\mathbf{F}$ of (5) are stated in [13] where, under natural geometric assumptions on the mesh, it is proved that, if the local scalar product $[\cdot,\cdot]_E$ is stable and consistent, then

$$\|\mathbf{F}^I - \mathbf{F}\|_{\mathbf{X}^h} \leqslant Ch\|p\|_{H^2(\Omega)}, \tag{9}$$

where $\mathbf{F}^I$ denotes the mimetic interpolant in $\mathbf{X}^h$ of the exact velocity field $\mathbf{u}$.

Let us assume, moreover, that

$$\|\mathscr{R}_E(\mathbf{G}^I) - \mathbf{v}\|_{L^2(E)} \leqslant Ch_E\|\mathbf{v}\|_{H^1(E)} \quad \forall \mathbf{v} \in H^1(E)^2,\ \forall E,$$

where $\mathbf{G}^I$ is the interpolant in $\mathbf{X}^h$ of $\mathbf{v}$. Then the following estimate for the pressure variable holds true

$$\|p - p^h\| \leqslant Ch\|p\|_{H^2(\Omega)}. \tag{10}$$

Remark 5. In [13] the error estimate for the pressure requires H^1 regularity of f. A careful analysis, however, shows that the optimal estimate (10) can be obtained (see [19]).

4. Mimetic modification of Raviart–Thomas elements on quadrilateral meshes

In this section, we make use of the theoretical framework discussed in the previous section for the analysis of a modification of RT element. The element we are going to present is analogous to the one which can be found in [25]. We denote the new element as MRT.

Let E be a quadrilateral of a mesh of the domain Ω and let $J(\hat{x},\hat{y}) = \alpha + \beta\hat{x} + \gamma\hat{y}$ be the Jacobian determinant of the bilinear mapping from the reference square $\widehat{E} = [0,1]^2$ to E. Let us define the vectorfield

$$\hat{b}_0(\hat{x},\hat{y}) = \begin{pmatrix} \frac{\beta\hat{x}(\hat{x}-1)}{2|E|} \\ \frac{\gamma\hat{y}(\hat{y}-1)}{2|E|} \end{pmatrix}$$

and consider the following four shape functions on the reference square $\hat{E}$:

$$\begin{aligned} \hat{b}_1(\hat{x},\hat{y}) &= |e_1|\begin{pmatrix} \hat{x}-1 \\ 0 \end{pmatrix} + |e_1|\hat{b}_0(\hat{x},\hat{y}), \\ \hat{b}_2(\hat{x},\hat{y}) &= |e_2|\begin{pmatrix} 0 \\ \hat{y}-1 \end{pmatrix} + |e_2|\hat{b}_0(\hat{x},\hat{y}), \\ \hat{b}_3(\hat{x},\hat{y}) &= |e_3|\begin{pmatrix} \hat{x} \\ 0 \end{pmatrix} + |e_3|\hat{b}_0(\hat{x},\hat{y}), \\ \hat{b}_4(\hat{x},\hat{y}) &= |e_4|\begin{pmatrix} 0 \\ \hat{y} \end{pmatrix} + |e_4|\hat{b}_0(\hat{x},\hat{y}). \end{aligned} \tag{11}$$

Remark 6. The function $\hat{b}_0$ is clearly equal to zero if E is a parallelogram (affine mapping) and has always zero normal components along the four sides of $\widehat{E}$ (i.e., $\hat{b}_0$ is a bubble in $H(\mathrm{div};\widehat{E})$). Notice that the four reference shape functions coincide with the standard RT ones in the case of affine mappings.

The actual shape functions on E are constructed from the reference ones, as usual, by using the Piola transform

$$\mathbf{v}(x,y) = \frac{1}{J(\hat{x},\hat{y})} DF(\hat{x},\hat{y})\,\hat{v}(\hat{x},\hat{y}), \quad (x,y) = F(\hat{x},\hat{y}), \tag{12}$$

where F is the bilinear mapping from $\widehat{E}$ to E.

The definition of the shape functions has been made in such a way that, for $\mathbf{v}$ in MRT, div$\mathbf{v}$ is always constant in each element (we recall that for standard RT elements this property is true only for affine meshes).

We now report the main steps for the analysis of the MRT elements.

The main link between this section and the previous one is that a lifting operator can be constructed by making use of MRT elements. This construction generalizes to quadrilaterals the RT-based lifting operator which is already known in the case of affine meshes.

Proposition 1. *The MRT-based lifting operator is P_0-compatible.*

Proof. Let us consider the shape functions on the reference square defined in (11). The basis functions on the current element obtained by means of the Piola transform are given by

$$b_i(x,y) = \frac{1}{J(\hat{x},\hat{y})} DF(\hat{x},\hat{y})\hat{b}_i(\hat{x},\hat{y}), \quad (x,y) = F(\hat{x},\hat{y})$$

and satisfy the following relations

$$\mathrm{div} b_{i|E} = \text{const.}, \quad b_i \cdot \mathbf{n}_{j_{|e_j}} = \delta_{ij}.$$

Therefore, the lifting operator $\mathscr{R}_E : \mathbf{X}_E^h \to L^2(E)$ can be defined as follows:

$$\mathscr{R}_E(\mathbf{G}) = \sum_{i=1}^{4} G_E^{e_i} b_i.$$

It is obvious that properties (1) and (2) in Definition 3 hold true. Let us now check property (3). We have to verify that constant vectors can be obtained as combination of the basis functions.

Let consider first the vector $\mathbf{c} = (1,0)^t$, we prove that it can be expressed as the Piola transform of a vector $\hat{\mathbf{c}}$ which is a suitable combination of the shape functions $\hat{b}_i$ on the reference element.

The bilinear mapping F from $\widehat{E}$ to E can be written as follows:

$$F(\hat{x},\hat{y}) = \begin{cases} a_1 + a_2\hat{x} + a_3\hat{y} + a_4\hat{x}\hat{y}, \\ b_1 + b_2\hat{x} + b_3\hat{y} + b_4\hat{x}\hat{y}, \end{cases}$$

hence it holds:

$$DF(\hat{x},\hat{y}) = \begin{pmatrix} a_2 + a_4\hat{y} & a_3 + a_4\hat{x} \\ b_2 + b_4\hat{y} & b_3 + b_4\hat{x} \end{pmatrix}.$$

Inverting the Piola transform (12), we obtain

$$\hat{\mathbf{c}} = JDF^{-1}\mathbf{c} = \begin{pmatrix} b_3 \\ -b_2 \end{pmatrix} + b_4\begin{pmatrix} \hat{x} \\ -\hat{y} \end{pmatrix}.$$

It is easy to check that

$$\begin{aligned} \hat{\mathbf{c}} = {} & \frac{b_3}{|e_1||e_3|}(|e_1|\hat{b}_3 - |e_3|\hat{b}_1) - \frac{b_2}{|e_2||e_4|}(|e_2|\hat{b}_4 - |e_4|\hat{b}_2) \\ & + \frac{b_4}{|e_3||e_4|}(|e_4|\hat{b}_3 - |e_3|\hat{b}_4). \end{aligned}$$

Analogously, if we take $\mathbf{c} = (0,1)^t$, we obtain that

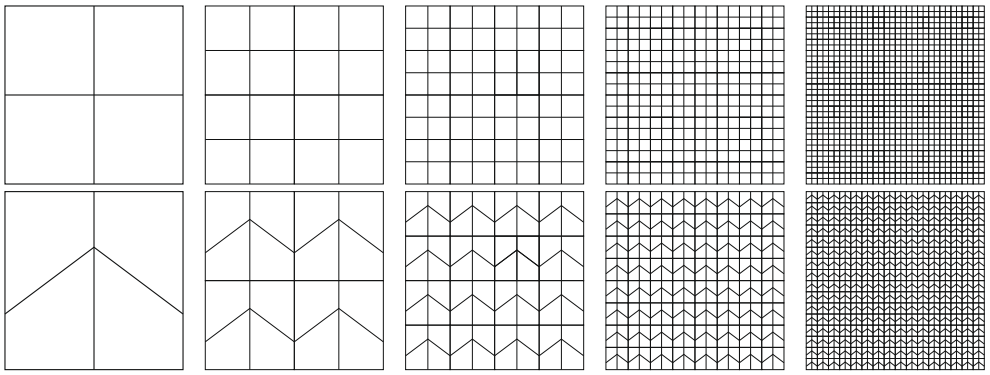

Fig. 1. Uniform meshes of squares and trapezoids.

Table 1
Square domain: eigenvalues computed with RT element on square mesh sequence.

Exact	Computed (rate)			
1.0	1.01292 (2.0)	1.00322 (2.0)	1.00080 (2.0)	1.00020 (2.0)
1.0	1.01292 (2.0)	1.00322 (2.0)	1.00080 (2.0)	1.00020 (2.0)
2.0	2.02583 (2.0)	2.00643 (2.0)	2.00161 (2.0)	2.00040 (2.0)
4.0	4.20955 (2.0)	4.05166 (2.0)	4.01287 (2.0)	4.00321 (2.0)
4.0	4.20955 (2.0)	4.05166 (2.0)	4.01287 (2.0)	4.00321 (2.0)
5.0	5.22246 (2.0)	5.05488 (2.0)	5.01367 (2.0)	5.00341 (2.0)
5.0	5.22246 (2.0)	5.05488 (2.0)	5.01367 (2.0)	5.00341 (2.0)
8.0	8.41909 (2.0)	8.10333 (2.0)	8.02573 (2.0)	8.00643 (2.0)
9.0	10.08029 (1.8)	9.26313 (2.0)	9.06524 (2.0)	9.01628 (2.0)
9.0	10.08029 (1.8)	9.26313 (2.0)	9.06524 (2.0)	9.01628 (2.0)
d.o.f.	144	544	2112	8320

$$\hat{\mathbf{c}} = \frac{-a_3}{|e_1||e_3|}(|e_1|\hat{b}_3 - |e_3|\hat{b}_1) + \frac{a_2}{|e_2||e_4|}(|e_2|\hat{b}_4 - |e_4|\hat{b}_2) - \frac{a_4}{|e_3||e_4|}(|e_4|\hat{b}_3 - |e_3|\hat{b}_4). \quad \square$$

According to the theory recalled in the previous section, the weighted $L^2(\Omega)$ scalar product induces a consistent definition of scalar product in the mimetic space $\mathbf{X}^h$ (see (4), (6) and (8)).

Proposition 2. *The scalar product associated with the MRT-based lifting operator is stable and consistent in the sense of (7) and (8).*

The consistency follows from the P_0-compatibility of the lifting, while the stability follows by the properties of the lifting operator, trace theorems, and scaling arguments.

Theorem 1. *Let* $(\mathbf{u}, p)$ *be the solution of (1) and* $(\mathbf{u}_h, p_h)$ *the corresponding solution of (2) obtained with the MRT scheme. Then the following optimal error estimates hold true*

$$\|\mathbf{u} - \mathbf{u}_h\|_{L^2(\Omega)} \leqslant Ch\|\mathbf{u}\|_{H^1(\Omega)},$$
$$\|\mathrm{div}(\mathbf{u} - \mathbf{u}_h)\|_{L^2(\Omega)} \leqslant Ch\|\mathrm{div}\mathbf{u}\|_{H^1(\Omega)},$$
$$\|p - p_h\|_{L^2(\Omega)} \leqslant Ch\|p\|_{H^2(\Omega)}.$$

The first estimate follows from the equivalence with mimetic finite differences and (9); the second one is an easy consequence of the fact that $\mathrm{div}\mathbf{u}_h$ turns out to be the L^2-projection of f onto Q_h; the third one can be obtained as a consequence of (10) in the framework of mimetic finite differences or by arguments analogous of the ones used in Theorem 11 of [1] in the framework of mixed finite elements.

5. Numerical results

In this section, we report on some numerical results related to the eigensolution to problem (3). We recall that we are solving the Darcy eigenvalue problem with Dirichlet boundary conditions.

Table 2
Square domain: eigenvalues computed with RT element on trapezoid mesh sequence.

Exact	Computed (rate)			
1.0	1.04839 (0.6)	1.04184 (0.2)	1.04022 (0.1)	1.03982 (0.0)
1.0	1.05311 (0.8)	1.04303 (0.3)	1.04052 (0.1)	1.03989 (0.0)
2.0	2.10100 (0.7)	2.08474 (0.3)	2.08071 (0.1)	2.07970 (0.0)
4.0	4.30128 (1.1)	4.19360 (0.6)	4.16738 (0.2)	4.16089 (0.1)
4.0	4.37659 (1.5)	4.21244 (0.8)	4.17211 (0.3)	4.16207 (0.1)
5.0	5.35150 (1.3)	5.23617 (0.6)	5.20777 (0.2)	5.20074 (0.0)
5.0	5.42319 (1.2)	5.25386 (0.7)	5.21220 (0.3)	5.20185 (0.1)
8.0	8.66877 (1.2)	8.40463 (0.7)	8.33900 (0.3)	8.32282 (0.1)
9.0	10.09193 (1.2)	9.53580 (1.0)	9.40108 (0.4)	9.36807 (0.1)
9.0	10.48030 (1.4)	9.63071 (1.2)	9.42497 (0.6)	9.37406 (0.2)
d.o.f.	144	544	2112	8320

Table 3
Square domain: eigenvalues computed with MRT element on square mesh sequence.

Exact	Computed (rate)			
1.0	1.01292 (2.0)	1.00322 (2.0)	1.00080 (2.0)	1.00020 (2.0)
1.0	1.01292 (2.0)	1.00322 (2.0)	1.00080 (2.0)	1.00020 (2.0)
2.0	2.02583 (2.0)	2.00643 (2.0)	2.00161 (2.0)	2.00040 (2.0)
4.0	4.20955 (2.0)	4.05166 (2.0)	4.01287 (2.0)	4.00321 (2.0)
4.0	4.20955 (2.0)	4.05166 (2.0)	4.01287 (2.0)	4.00321 (2.0)
5.0	5.22246 (2.0)	5.05488 (2.0)	5.01367 (2.0)	5.00341 (2.0)
5.0	5.22246 (2.0)	5.05488 (2.0)	5.01367 (2.0)	5.00341 (2.0)
8.0	8.41909 (2.0)	8.10333 (2.0)	8.02573 (2.0)	8.00643 (2.0)
9.0	10.08029 (1.8)	9.26313 (2.0)	9.06524 (2.0)	9.01628 (2.0)
9.0	10.08029 (1.8)	9.26313 (2.0)	9.06524 (2.0)	9.01628 (2.0)
d.o.f.	144	544	2112	8320

Given a finite element space $\mathbf{V}_h \subset \mathbf{V}$, the discretization of (3) reads: find $\lambda_h \in \mathbb{R}$ and $\mathbf{u}_h \in \mathbf{V}_h$ with $\mathbf{u}_h \neq 0$ such that

$$(\mathrm{div}\mathbf{u}_h, \mathrm{div}\mathbf{v}) = \lambda_h(\mathbb{K}^{-1}\mathbf{u}_h, \mathbf{v}) \quad \forall \mathbf{v} \in \mathbf{V}_h. \tag{13}$$

As it has been already observed, the eigensolution of (13) are exactly the same as those of the discretization of the eigenvalue problem associated with (1) if $Q_h = \mathrm{div}\mathbf{V}_h$. In particular, this equivalence is not true on general quadrilateral meshes if one uses the standard lowest-order RT element and Q_h made of piecewise constant functions. We shall report the results already presented in [12] showing that the eigenvalues computed with lowest-order RT element do not converge.

With the modified space MRT, however, the equivalence is true since $\mathrm{div}\mathbf{v}$ is constant on each element whenever $\mathbf{v}$ belongs to MRT. Then, the estimates of Theorem 1 guarantee that we can use the theory of Boffi et al. [8] and Babuška and Osborn [2] in order to prove the convergence of the eigensolutions. Our numerical results confirm the theoretical analysis.

In the numerical tests we take for simplicity $\mathbb{K}$ to be the identity matrix (it is not difficult to see that in this case our problem corresponds to Laplace eigenvalue problem with Neumann boundary conditions). The domain is the square $[0, \pi]^2$ or an L-shaped domain; we are using two mesh sequences: a uniform mesh of squares and a uniform mesh of distorted trapezoids as in [1] (see Fig. 1 for the mesh sequences on the square domain). The reported computations are performed with a refinement level ranging from 8 to 64.

In the case of the square domain, we report in Tables 1 and 2 the approximation of the first 10 positive eigenvalues of problem (3) together with the rates of convergence obtained by standard RT element on the mesh sequence of squares and trapezoids, respectively.

It is clear that, on distorted quadrilaterals, standard RT element does not converge. Actually, it can be shown that the computed

Table 4
Square domain: eigenvalues computed with MRT element on trapezoid mesh sequence.

Exact	Computed (rate)			
1.0	1.00986 (2.0)	1.00246 (2.0)	1.00061 (2.0)	1.00015 (2.0)
1.0	1.01315 (2.0)	1.00328 (2.0)	1.00082 (2.0)	1.00020 (2.0)
2.0	2.02406 (2.0)	2.00603 (2.0)	2.00151 (2.0)	2.00038 (2.0)
4.0	4.15955 (2.0)	4.03943 (2.0)	4.00982 (2.0)	4.00245 (2.0)
4.0	4.21334 (2.5)	4.05261 (2.0)	4.01310 (2.0)	4.00327 (2.0)
5.0	5.17562 (1.9)	5.04382 (2.0)	5.01094 (2.0)	5.00273 (2.0)
5.0	5.22645 (2.3)	5.05622 (2.0)	5.01402 (2.0)	5.00350 (2.0)
8.0	8.37993 (1.8)	8.09640 (2.0)	8.02411 (2.0)	8.00603 (2.0)
9.0	9.81517 (1.6)	9.20071 (2.0)	9.04980 (2.0)	9.01242 (2.0)
9.0	10.09560 (1.7)	9.26795 (2.0)	9.06644 (2.0)	9.01657 (2.0)
d.o.f.	144	544	2112	8320

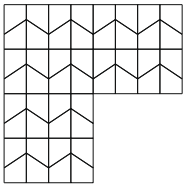

Fig. 2. Distorted mesh for the L-shaped domain.

eigenvalues converge optimally towards wrong values which depend upon the distortion of the mesh.

Tables 3 and 4 show the corresponding results for the modified MRT element.

It is evident that in this case optimal convergence is achieved also on distorted meshes. Of course, the results on the square mesh sequence coincide with those of RT since in this case the modification does not occur.

In the case of the L-shaped domain, the reference solution is not known analytically. For this reason, we used the domain and the reference solution proposed in the web page [18] (example 2DomA) where the eigenvalues are computed with an accuracy of 11 significant digits. The corners of the domain are located at $(0,0)$, $(1,0)$, $(1,1)$, $(-1,1)$, $(-1,-1)$, $(0,-1)$. Fig. 2 shows the distorted mesh with refinement level equal to 8.

The results of the computations performed with the MRT element are reported in Table 5.

The lower rate of convergence of the first eigenvalue reflects the fact that the corresponding eigenfunction is not smooth. This is in perfect agreement with the expected results and confirms that the method is performing well also on a nonconvex domain.

6. Concluding remarks

We presented the equivalence between the modified RT element proposed in [25] and a P_0-compatible lifting for the mimetic finite differences scheme. The modification (which is only active on distorted quadrilateral meshes) restores optimal convergence on non-affine meshes. Numerical tests on a model eigenvalue problem confirm the theoretical results. In particular, it is apparent that lowest-order RT element does not achieve eigenvalue convergence on non-affine meshes.

Table 5
L-shaped domain: eigenvalues computed with MRT element on trapezoid mesh sequence.

Exact	Computed (rate)			
1.47562	1.46136 (0.4)	1.46819 (0.9)	1.47222 (1.1)	1.47416 (1.2)
3.53403	3.58598 (2.1)	3.54650 (2.1)	3.53707 (2.0)	3.53478 (2.0)
9.86960	10.26323 (2.0)	9.96689 (2.0)	9.89384 (2.0)	9.87565 (2.0)
9.86960	10.39599 (2.5)	9.99942 (2.0)	9.90194 (2.0)	9.87767 (2.0)
11.38948	11.86458 (2.0)	11.50780 (2.0)	11.41894 (2.0)	11.39682 (2.0)
d.o.f.	112	416	1600	6272

Table 6
Approximation rates for lowest-order RT, MRT and ABF elements. Order of convergence for eigenvalues of problem (13).

Spaces	$\|\mathbf{u}-\mathbf{u}^I\|_{L^2(\Omega)}$		$\|\mathrm{div}(\mathbf{u}-\mathbf{u}^I)\|_{L^2(\Omega)}$		$\|\lambda-\lambda_h\|$	
	Affine	Distorted	Affine	Distorted	Affine	Distorted
RT	1	1	1	0	2	0
ABF	1	1	2	1	2	2
MRT	1	1	1	1	2	2

Table 7
Approximation rates for BDM_k, BDFM_{k+1}, RT_k and ABF_k elements ($k \geqslant 1$).

Spaces	$\|\mathbf{u}-\mathbf{u}^I\|_{L^2(\Omega)}$		$\|\mathrm{div}(\mathbf{u}-\mathbf{u}^I)\|_{L^2(\Omega)}$	
	Affine	Distorted	Affine	Distorted
BDM_k	$k+1$	$\lfloor\frac{k+1}{2}\rfloor$	k	$\lfloor\frac{k}{2}\rfloor$
BDFM_{k+1}	$k+1$	$\lfloor\frac{k+2}{2}\rfloor$	$k+1$	$\lfloor\frac{k+1}{2}\rfloor$
RT_k	$k+1$	$k+1$	$k+1$	k
ABF_k	$k+1$	$k+1$	$k+2$	$k+1$

The developed theory could be also interpreted in the framework of locally conservative discretization methods for the approximation of Darcy's law. We refer the interested reader to Cai et al. [17] and Klausen and Russell [22] for more details on this subject and for possible connections with control volume techniques.

For the reader convenience, we summarize the approximation properties of the most popular finite element discretizations of $H(\mathrm{div};\Omega)$. The presented tables are essentially a clarification of the consequences of Arnold et al. [1] and should make it clear the importance of the present investigation. The three-dimensional picture is even more problematic and will be the object of future study.

Table 6 refers to the lowest-order approximation that we discussed in the present paper: RT and MRT. We included also the lowest-order member of the ABF family presented in [1].

Here $\mathbf{u}^I$ denotes the interpolant of $\mathbf{u}$. It is clear that the MRT choice provides optimal approximation rates with the least effort, while RT element does not converge on general meshes. ABF element, on the other hand, is the optimal theoretical choice in the framework of classical implementation (i.e., the reference space does not depend on the mapping); however, it involves additional degrees of freedom with an additional computational cost.

For the sake of completeness, Table 7 summarizes the approximation properties of the higher-order spaces of the families BDM, BDFM, RT, and ABF. The subscript k is related to the polynomial degrees. We recall that the following inclusions hold ($k \geqslant 1$):

$$\mathrm{BDM}_k \subset \mathrm{BDFM}_{k+1} \subset \mathrm{RT}_k \subset \mathrm{ABF}_k$$

and that BDFM_1 coincides with RT_0 (we are keeping the index shift in the definition of BDFM for historical reasons). With this notation, the spaces of Table 6 correspond to the choice $k=0$ (note that BDM_0 does not exist).

It is clear that ABF is the only optimally convergent family on distorted meshes; RT is suboptimally convergent by one order in the divergence, while the approximation rates for BDM and BDFM are basically reduced by one half on distorted meshes.

References

[1] Arnold DN, Boffi D, Falk RS. Quadrilateral $H(\mathrm{div})$ finite elements. SIAM J Numer Anal 2005;42(6):2429–51 [electronic].
[2] Babuška I, Osborn J. Eigenvalue problems. In: Ciarlet P, Lions J, editors. Handbook of numerical analysis, vol. 2. North Holland: Elsevier Science Publishers B.V.; 1991. p. 641–788.
[3] Bathe K-J, Nitikitpaiboon C, Wang X. A mixed displacement-based finite element formulation for acoustic fluid–structure interaction. Comput Struct 1995;56(2–3):225–37.
[4] Bermúdez A, Gamallo P, Nogueiras MR, Rodríguez R. Approximation of a structural acoustic vibration problem by hexahedral finite elements. IMA J Numer Anal 2006;26(2):391–421.
[5] Bermúdez I, Durán R, Muschietti A, Rodríguez R, Solomin J. Finite element vibration analysis of fluid–solid systems without spurious modes. SIAM J Numer Anal 1995;32:1280–95.
[6] Berndt M, Lipnikov K, Moulton D, Shashkov M. Convergence of mimetic finite difference discretizations of the diffusion equation. East–West J Numer Math 2001;9(4):265–84.
[7] Berndt M, Lipnikov K, Shashkov M, Wheeler MF, Yotov I. Superconvergence of the velocity in mimetic finite difference methods on quadrilaterals. SIAM J Numer Anal 2005;43(4):1728–49 [electronic].
[8] Boffi D, Brezzi F, Gastaldi L. On the convergence of eigenvalues for mixed formulations. Ann Scuola Norm Sup Pisa Cl Sci (4) 1997;25(1–2):131–54 [Dedicated to Ennio De Giorgi].

[9] Boffi D, Chinosi C, Gastaldi L. Approximation of the grad div operator in nonconvex domains. CMES Comput Model Eng Sci 2000;1(2):31–43.
[10] Boffi D, Fernandes P, Gastaldi L, Perugia I. Computational models of electromagnetic resonators: analysis of edge element approximation. SIAM J Numer Anal 1999;36(4):1264–90.
[11] Boffi D, Gastaldi L. Mimetic finite differences and quadrilateral mixed finite elements, in preparation.
[12] Boffi D, Kikuchi F, Schöberl J. Edge element computation of Maxwell's eigenvalues on general quadrilateral meshes. Math Model Method Appl Sci 2006;16(2):265–73.
[13] Brezzi F, Lipnikov K, Shashkov M. Convergence of the mimetic finite difference method for diffusion problems on polyhedral meshes. SIAM J Numer Anal 2005;43(5):1872–96 [electronic].
[14] Brezzi F, Lipnikov K, Shashkov M. Convergence of mimetic finite difference method for diffusion problems on polyhedral meshes with curved faces. Math Model Method Appl Sci 2006;16(2):275–97.
[15] Brezzi F, Lipnikov K, Shashkov M, Simoncini V. A new discretization methodology for diffusion problems on generalized polyhedral meshes. Comput Method Appl Mech Eng. 2007;196(37–40):3682–92.
[16] Brezzi F, Lipnikov K, Simoncini V. A family of mimetic finite difference methods on polygonal and polyhedral meshes. Math Model Method Appl Sci 2005;15(10):1533–51.
[17] Cai Z, Jones JE, McCormick SF, Russell TF. Control-volume mixed finite element methods. Comput Geosci 1997;1(3–4):289–315.
[18] Dauge M. Benchmark computations for Maxwell equations. <http://perso.univ-rennes1.fr/monique.dauge/benchmax.html>.
[19] Gardini F. Personal communication.
[20] Gastaldi L. Mixed finite element methods in fluid–structure systems. Numer Math 1996;74(2):153–76.
[21] Hyman JM, Shashkov M. The orthogonal decomposition theorems for mimetic finite difference methods. SIAM J Numer Anal 1999;36(3):788–818 [electronic].
[22] Klausen RA, Russell TF. Relationships among some locally conservative discretization methods which handle discontinuous coefficients. Comput Geosci 2004;8(4):341–77.
[23] Kuznetsov Y, Repin S. Convergence analysis and error estimates for mixed finite element method on distorted meshes. J Numer Math 2005;13(1):33–51.
[24] Shashkov M. Conservative finite-difference methods on general grids. Symbolic and numeric computation series. Boca Raton, FL: CRC Press; 1996 [With 1 IBM-PC floppy disk 3.5 in.; HD].
[25] Shen J. Mixed finite element methods on distorted rectangular grids. Technical report, ISC-94-13-MATH, Texas A&M University; 1994.
[26] Wang X, Bathe K-J. Displacement/pressure based mixed finite element formulations for acoustic fluid–structure interaction problems. Int J Numer Method Eng 1997;40:2001–17.
[27] Wang X, Bathe K-J. On mixed elements for acoustic fluid–structure interactions. Math Model Method Appl Sci 1997;7(3):329–43.